ELSEVIER

Available at WWW.MATHEMATICSWEB.ORG POWERED BY SCIENCE DIRECT®

Applied Numerical Mathematics 43 (2002) 459–481

APPLIED NUMERICAL MATHEMATICS

www.elsevier.com/locate/apnum

Fine tuning interface relaxation methods for elliptic differential equations ☆

J.R. Rice *, P. Tsompanopoulou, E. Vavalis [1]

Purdue University, Computer Science Department, West Lafayette, IN 47907, USA

Abstract

Two simple interface relaxation techniques for solving elliptic differential equations are considered. A theoretical analysis is carried out at the differential level and "optimal" relaxation parameters are obtained for model problems. A comprehensive experimental numerical study for 1- and 2-dimensional problems is also presented. We present a complete analysis of convergence and optimum parameters for two 1-dimensional methods applied to Helmholtz equations: the averaging method **AVE** and the Robin-type method **ROB**. We then present experimental studies for 1- and 2-dimensional methods and more general equations. These studies confirm the theoretical results and suggest they are valid in these more general cases.

1. Introduction

Domain decomposition has proven an effective means of partitioning the task of solving Differential Equation (DE) problems numerically. It is mainly an algebraic approach and works by splitting the discrete DE domain into subdomains which can be coupled in many ways. The well established additive and multiplicative Schwartz methods are examples of typical domain decomposition approaches that have been analyzed extensively. Interface Relaxation (IR) is a step beyond domain decomposition [14]. IR methods are defined and analyzed at the continuous level, yet they can be implemented by traditional numerical methods which can vary from subdomain to subdomain. They assume a splitting of the domain into a set of non-overlapping subdomains and consider the associated DE problems defined on each one

☆ Work supported in part by PENED grants 95-602 and 95-107, NSF grants CCR-9202536 and CDA-9123502, and AFOSR FM 49620-92-J-0069.

* Corresponding author.
E-mail address: jrr@cs.purdue.edu (J.R. Rice).

[1] Author's permanent address: University of Crete, Mathematics Department, 714 09 Heraklion, Greece and IACM, FORTH, 711 10 Heraklion, Greece.

0168-9274/02/$22.00
PII: S0168-9274(01)00176-3

of them. These subproblems are coupled through relaxation mechanisms on the interfaces. IR methods naturally apply to multi-physics problems when the DE may change from one subdomain to another. For a general introduction to the IR methodology the reader is referred to [14,11,12].

Several interface relaxation methods, considered form the domain decomposition viewpoint, like the Schwartz method, the Poincaré–Steklov method, the Schur complement, can be found in [1,2,18,19,23]. A review of a large collection of IR methods is presented in [13]. The convergence of these schemes depends, as expected, on the differential operator, on the geometry of the original domain, and on the geometry of the subdomains chosen. This makes the selection of "optimum" values for the relaxation parameters a hard and challenging problem. On the other hand, the local subdomain discretization scheme does not affect the convergence properties of the IR schemes which gives these methods great versatility; one can select the most appropriate discretization parameters or numerical method for the differential problem defined on each subdomain.

The development of an automated and adaptive procedure that dynamically estimates "good" relaxation parameters, using automatic differentiation techniques, for general differential operators and arbitrarily shaped subdomains is under way [16]. Nevertheless, in order for this parameter selection procedure to be effective, theoretical results for simple model problems are needed that provide the required reasonably good initial guess for the optimum values of the parameters and, more importantly, a better understanding of the convergence mechanisms involved.

The main objective of this paper is to better understand IR methods for model problems where direct analysis can be made. In particular, we analytically estimate values for the parameters involved in two recently proposed and analyzed IR methods. Namely, we consider an averaging scheme [17,24, 25] (denoted by **AVE** in the sequel) and a Robin-type IR scheme [10] (denoted by **ROB**). In [17], Fourier analysis is applied for the theoretical analysis and shows that the fast convergence rate of the **AVE** method in the case of constant coefficients and rectangular subdomains. the theoretical results are verified by the experimental ones. In [24], a convergence analysis of the **AVE** method is carried out at differential level using Hilbert space techniques. Numerical experiments verify the fast convergence of the method and its stability with respect to different decompositions and different problems, using constant relaxation parameters. In [25] a very closely related method to **AVE** is considered. The theoretical analysis is done by Galerkin approximation with Lagrange multipliers and a mixed finite element method, and shows that the error is independent of the grid size. These results are checked through numerical experiments. The **ROB** method is formulated and analyzed in [10] for the Laplace equation. Convergence is proved through energy norms, though there are no estimates of good relaxation parameter values to accelerate the convergence. Although both methods were analyzed in these studies, more understanding is needed. Specifically, expressions that relate their rate of convergence to the characteristics of the differential problem and its partition in a clear way are needed.

The theoretical study in this paper concerns only one-dimensional boundary value problems. Nevertheless, it seems to us that it is possible to extend this work to two-dimensions following the framework used in [6]. Such an extension is beyond the scope of the present study.

We restrict ourselves to Helmholtz boundary value problems. In both schemes the error involved on each interface can be given analytically in terms of the error in the previous iteration. This leads us to a system of linear algebraic equations that represents the relation between the errors on all interfaces in two consequent iterations. Then, we minimize the spectral radius of the iteration matrix involved using a different approach for each method. For the **AVE** scheme we minimize the area of the associated Gerschgorin discs (which is equivalent of bounding the max norm of the iteration matrix) to derive, in

Theorem 4, an important relation between the size of the subdomains and the coefficient of the differential equation that determines the domain of convergence of the method.

The iteration matrix associated with the **ROB** scheme is quite sparse, and so we were able to make its spectral radius zero by selecting appropriate values for the relaxation parameters involved. In particular, Theorem 3 gives optimum values of the relaxation parameters involved, which are proved to be independent both of the particular discretization of the differential operator and its original domain.

The rest of this paper is organized as follows. In Section 2 we formulate the two Interface Relaxation methods whose theoretical convergence analysis is given in Section 3. Section 4 presents numerical results from an experimental study which confirm our theoretical results; they also show that these hold for more general problems, including two dimensional ones.

2. Two interface relaxation methods

We consider the Helmholtz boundary value problem

$$Lu \equiv -u''(x) + \gamma^2(x)u(x) = f(x), \quad x \in \Omega \equiv (a,b), \tag{1}$$

with $a, b \in \mathbb{R}$, subject to boundary conditions on a and b which, for simplicity, are taken to be homogeneous Dirichlet. Assume that Ω is decomposed into the p non-overlapping subdomains

$$\Omega_i \equiv (x_{i-1}, x_i), \quad i = 1, \ldots, p$$

with $x_0 = a,\ x_p = b$ and $x_{i-1} < x_i \in \Omega$ for $i = 1, \ldots, p-1$. We denote the size of a subdomain Ω_i by $\ell_i = x_i - x_{i-1}$ and the restrictions of L, f and γ in Ω_i by L_i, f_i, γ_i, respectively. We further assume that $\gamma(x) = \gamma_i$ for $x \in \Omega_i,\ i = 1, \ldots, p$, where the γ_i's are real constants.

2.1. The *ROB* method

The **ROB** method is defined, for the model problem under consideration, by the following algorithm:

(1) Define:

$$\left.\begin{aligned} g_i^i &= \left.\frac{du_{i+1}^{(k)}}{dx}\right|_{x=x_i} + \lambda_i u_{i+1}^{(k)}\big|_{x=x_i} \\ g_i^{i+1} &= -\left.\frac{du_i^{(k)}}{dx}\right|_{x=x_i} + \lambda_i u_i^{(k)}\big|_{x=x_i} \end{aligned}\right\} \quad i = 1, \ldots, p-1.$$

(2) Choose initial guesses $u_i^{(0)}(x)$ for the solutions on each subdomain $\Omega_i,\ i = 1, 2, \ldots, p$.

(3) Define the sequence of subdomain solutions $u_i^{(k)}(x),\ k = 1, 2, \ldots$ as follows:

$$\left.\begin{aligned} &L_1 u_1^{(k+1)} = f_1 \quad \text{in } \Omega_1 \\ &u_1^{(k+1)}\big|_{x=x_0} = 0 \\ &\left.\frac{du_1^{(k+1)}}{dx}\right|_{x=x_1} + \lambda_1 u_1^{(k+1)}\big|_{x=x_1} = g_1^1 \end{aligned}\right| \left.\begin{aligned} &L_p u_p^{(k+1)} = f_p \quad \text{in } \Omega_p \\ &-\left.\frac{du_p^{(k+1)}}{dx}\right|_{x=x_{p-1}} + \lambda_{p-1} u_p^{(k+1)}\big|_{x=x_{p-1}} = g_{p-1}^p \\ &u_p^{(k+1)}\big|_{x=x_p} = 0 \end{aligned}\right.$$

$$\left.\begin{aligned} & L_i u_i^{(k+1)} = f_i \quad \text{in } \Omega_i \\ & -\frac{du_i^{(k+1)}}{dx}\bigg|_{x=x_{i-1}} + \lambda_{i-1} u_i^{(k+1)}\big|_{x=x_{i-1}} = g_{i-1}^i \\ & \frac{du_i^{(k+1)}}{dx}\bigg|_{x=x_i} + \lambda_i u_i^{(k+1)}\big|_{x=x_i} = g_i^i \end{aligned}\right\} \quad i = 2, \ldots, p-1.$$

This method is based on a simple relaxation technique that involves the Robin interface conditions shown above. The DE problem is solved in each subdomain where the boundary conditions are provided from the previously computed solution and its outward normal derivative from the adjacent subdomains. The *relaxation parameter* λ_i controls the influence of the value of the function and its normal derivative on the smoothing Robin interface conditions.

This method was first proposed and analyzed in [10] where, through energy estimates, the convergence of the method at differential level was established for arbitrary decompositions and elliptic operators. Later in [5,8], this method was further analyzed at discrete level in a finite element framework. Several variations of this method have been also appeared. In [7] an ADI based modification is considered and analyzed at discrete level for model problems and decompositions. A second variation of the **ROB** method that extends its applicability and frees it from the cross-point trouble is formulated and analyzed in [4]. In [21] the addition of tangential derivatives in the smoothing procedure is proposed and analyzed and, recently, in [26] a finite difference variation is presented and analyzed. In some of these studies optimal values for the relaxation parameters have been obtained but only for model problems and only assuming a discrete formulation of the method (i.e., first discretize and then decompose the linear algebra problem). Therefore the determination of effective choices for λ_i's in the IR framework and for general domains and decompositions is, *in general, an open problem*.

*2.2. The two-step average **AVE** method*

The **AVE** IR method [13,17,24,25] is a two-step iterative scheme described by the following algorithm:

(1) Choose initial guesses $u_i^{(0)}(x)$ for the solution on each subdomain Ω_i, $i = 1, 2, \ldots, p$.
(2) Define the odd terms of the sequence of subdomain solutions $u_i^{(2k+1)}(x)$ as follows:

$$g_i^i = \beta_i \frac{du_i^{(2k)}}{dx}\bigg|_{x=x_i} + (1-\beta_i)\frac{du_{i+1}^{(2k)}}{dx}\bigg|_{x=x_i}, \quad i = 1, \ldots, p-1.$$

$$\begin{array}{l|l|l} & \text{for } i = 2, \ldots, p-1 & \\ L_1 u_1^{(2k+1)} = f_1 \quad \text{in } \Omega_1 & L_i u_i^{(2k+1)} = f_i \quad \text{in } \Omega_i & L_p u_p^{(2k+1)} = f_p \quad \text{in } \Omega_p \\ u_1^{(2k+1)}\big|_{x=x_0} = 0 & \dfrac{du_i^{(2k+1)}}{dx}\bigg|_{x=x_{i-1}} = g_{i-1}^{i-1} & \dfrac{du_p^{(2k+1)}}{dx}\bigg|_{x=x_{p-1}} = g_{p-1}^{p-1} \\ \dfrac{du_1^{(2k+1)}}{dx}\bigg|_{x=x_1} = g_1^1 & \dfrac{du_i^{(2k+1)}}{dx}\bigg|_{x=x_i} = g_i^i & u_p^{(2k+1)}\big|_{x=x_p} = 0. \end{array}$$

(3) Define the even terms of the sequence of subdomain solution $u_i^{(2k+2)}(x)$ as follows:

$$h_i^i = \alpha_i u_i^{(2k+1)}\big|_{x=x_i} + (1-\alpha_i)u_{i+1}^{(2k+1)}\big|_{x=x_i}, \quad i = 1,\dots,p-1.$$

$$\begin{array}{l|l|l}
L_1 u_1^{(2k+2)} = f_1 \quad \text{in } \Omega_1 & \text{for } i = 2,\dots,p-1 & L_p u_p^{(2k+2)} = f_p \quad \text{in } \Omega_p \\
u_1^{(2k+2)}\big|_{x=x_0} = 0 & L_i u_i^{(2k+2)} = f_i \quad \text{in } \Omega_i & u_p^{(2k+2)}\big|_{x=x_{p-1}} = h_{p-1}^{p-1} \\
u_1^{(2k+2)}\big|_{x=x_1} = h_1^1 & u_i^{(2k+2)}\big|_{x=x_{i-1}} = h_{i-1}^{i-1} & u_p^{(2k+2)}\big|_{x=x_p} = 0. \\
 & u_i^{(2k+2)}\big|_{x=x_i} = h_i^i &
\end{array}$$

The relaxation parameters α_i and β_i are to smooth the function and its normal derivative, respectively, and they both take values in $(0,1)$. In the first step (odd terms), the Neumann problem is solved for each subdomain, using as estimates of the derivatives on the interface a convex combination of the normal derivatives of the initial guess (or previously computed solutions). Then a convex combination of the values of computed solutions on adjacent domains is computed and used as boundary values to solve the Dirichlet problem in the second step (even terms). There are already several theoretical results concerning the **AVE** method. In [25], two finite element approaches (a Galerkin and a hybrid mixed) have been employed to analyze the convergence of the method at a discrete level setting both relaxation parameters equal to $1/2$. A convergence analysis of the method at the differential level using Hilbert space techniques is given in [24]. A simple model problem with a two subdomain decomposition is considered in [17] where Fourier analysis at the differential level is used to obtain "good" values for the interface relaxation parameter β_1, while α_1 is set equal to $1/2$.

It is worth pointing out the inherent parallelism in both the algorithms. In each one the DE solver or interface task steps can be executed on different processing elements. The only synchronization needed is a barrier at the end of each step and then only data on the interfaces need to be communicated to the processors handling neighboring subdomains. Note that parallelism and the number of subdomain are somewhat separate issues. One can apply IR to a problem with k subdomains using one, k or any number of processors in-between.

3. Selection of relaxation parameters

We start our analysis by stating the following simple lemma that can be easily verified.

Lemma 1. *The solution of the boundary value problem*

$$Lu = 0 \quad \text{in } (a,b), \qquad c_1 u'(a) + c_2 u(a) = v_1 \quad \text{and} \quad c_3 u'(b) + c_4 u(b) = v_2$$

with constants $c_i \in \mathbb{R}$, $i = 1,2,3,4$, is given by

$$\begin{aligned}
u(x) = {} & \big[\big(-(c_3\gamma + c_4)e^{\gamma(b-x)} + (-c_3\gamma + c_4)e^{-\gamma(b-x)}\big)v_1 \\
& + \big(-(-c_1\gamma + c_2)e^{\gamma(x-a)} + (c_1\gamma + c_2)e^{-\gamma(x-a)}\big)v_2\big] \\
& \times \big[(c_1\gamma + c_2)(-c_3\gamma + c_4)e^{-\gamma(b-a)} - (c_3\gamma + c_4)(-c_1\gamma + c_2)e^{\gamma(b-a)}\big]^{-1}. \qquad (2)
\end{aligned}$$

Let us now introduce notation for the sequence of values of the solutions, their derivatives and their errors at the interface points: $u_{i,j}^{(k)} \equiv u_i^{(k)}(x_j)$, $du_{i,j}^{(k)} \equiv \frac{du_i^{(k)}}{dx}\big|_{x=x_j}$, $\varepsilon_i^{(k)}(x) \equiv u_i^{(k)}(x) - u(x)$, $\varepsilon_{i,j}^{(k)} \equiv u_{i,j}^{(k)} - u(x_j)$ and $d\varepsilon_{i,j}^{(k)} \equiv du_{i,j}^{(k)} - u'(x_j)$.

3.1. Optimum relaxation parameters for the **ROB** method

Consider the following differential problems associated with the error functions in each subdomain which can be easily obtained from the **ROB** algorithm given in the previous section.

$$\begin{aligned} &L_1\varepsilon_1^{(k+1)}(x) = 0, \quad x \in \Omega_1,\\ &\varepsilon_{1,0}^{(k+1)} = 0, \qquad d\varepsilon_{1,1}^{(k+1)} + \lambda_1\varepsilon_{1,1}^{(k+1)} = d\varepsilon_{2,1}^{(k)} + \lambda_1\varepsilon_{2,1}^{(k)}, \end{aligned} \tag{3}$$

for $i = 2, \ldots, p-1$,

$$\begin{aligned} &L_i\varepsilon_i^{(k+1)}(x) = 0, \quad x \in \Omega_i,\\ &-d\varepsilon_{i,i-1}^{(k+1)} + \lambda_{i-1}\varepsilon_{i,i-1}^{(k+1)} = -d\varepsilon_{i-1,i-1}^{(k)} + \lambda_{i-1}\varepsilon_{i-1,i-1}^{(k)},\\ &d\varepsilon_{i,i}^{(k+1)} + \lambda_i\varepsilon_{i,i}^{(k+1)} = d\varepsilon_{i+1,i}^{(k)} + \lambda_i\varepsilon_{i+1,i}^{(k)}, \end{aligned} \tag{4}$$

$$\begin{aligned} &L_p\varepsilon_p^{(k+1)}(x) = 0, \quad x \in \Omega_p,\\ &-d\varepsilon_{p,p-1}^{(k+1)} + \lambda_{p-1}\varepsilon_{p,p-1}^{(k+1)} = -d\varepsilon_{p-1,p-1}^{(k)} + \lambda_{p-1}\varepsilon_{p-1,p-1}^{(k)}, \qquad \varepsilon_{p,p}^{(k+1)} = 0. \end{aligned} \tag{5}$$

Using (2) we observe that these error functions are given by

$$\varepsilon_1^{(k+1)}(x) = \frac{-e^{\gamma_1(x-x_0)} + e^{-\gamma_1(x-x_0)}}{(-\gamma_1+\lambda_1)e^{-\gamma_1\ell_1} - (\gamma_1+\lambda_1)e^{\gamma_1\ell_1}}\big(d\varepsilon_{21}^{(k)} + \lambda_1\varepsilon_{21}^{(k)}\big), \tag{6}$$

for $i = 2, \ldots, p-1$,

$$\begin{aligned} \varepsilon_i^{(k+1)}(x) = {} & \big[(-\gamma_i+\lambda_{i-1})(-\gamma_i+\lambda_i)e^{-\gamma_i\ell_i} - (\gamma_i+\lambda_i)(\gamma_i+\lambda_{i-1})e^{\gamma_i\ell_i}\big]^{-1}\\ &\times\Big[\big(-(\gamma_i+\lambda_i)e^{\gamma_i(x_i-x)} + (-\gamma_i+\lambda_i)e^{-\gamma_i(x_i-x)}\big)\big(-d\varepsilon_{i-1,i-1}^{(k)} + \lambda_{i-1}\varepsilon_{i-1,i-1}^{(k)}\big)\\ &+\big(-(\gamma_i+\lambda_{i-1})e^{\gamma_i(x-x_{i-1})} + (-\gamma_i+\lambda_{i-1})e^{-\gamma_i(x-x_{i-1})}\big)\big(d\varepsilon_{i+1,i}^{(k)} + \lambda_i\varepsilon_{i+1,i}^{(k)}\big)\Big] \end{aligned} \tag{7}$$

and

$$\varepsilon_p^{(k+1)}(x) = \frac{-e^{\gamma_p(x_p-x)} + e^{-\gamma_p(x_p-x)}}{(-\gamma_p+\lambda_{p-1})e^{-\gamma_p\ell_p} - (\gamma_p+\lambda_{p-1})e^{\gamma_p\ell_p}}\big(-d\varepsilon_{p-1,p-1}^{(k)} + \lambda_{p-1}\varepsilon_{p-1,p-1}^{(k)}\big). \tag{8}$$

From these we obtain

$$\begin{aligned} \varepsilon_{1,1}^{(k+1)} &= \frac{m_1}{\gamma_1 n_1 + \lambda_1 m_1}\big(d\varepsilon_{2,1}^{(k)} + \lambda_1\varepsilon_{2,1}^{(k)}\big),\\ \varepsilon_{i,i-1}^{(k+1)} &= \frac{1}{d_i}\big[(\gamma_i n_i + \lambda_i m_i)\big(-d\varepsilon_{i-1,i-1}^{(k)} + \lambda_{i-1}\varepsilon_{i-1,i-1}^{(k)}\big) + 2\gamma_i\big(d\varepsilon_{i+1,i}^{(k)} + \lambda_i\varepsilon_{i+1,i}^{(k)}\big)\big],\\ \varepsilon_{i,i}^{(k+1)} &= \frac{1}{d_i}\big[(\gamma_i n_i + \lambda_{i-1} m_i)\big(d\varepsilon_{i+1,i}^{(k)} + \lambda_i\varepsilon_{i+1,i}^{(k)}\big) + 2\gamma_i\big(-d\varepsilon_{i-1,i-1}^{(k)} + \lambda_{i-1}\varepsilon_{i-1,i-1}^{(k)}\big)\big],\\ \varepsilon_{p,p-1}^{(k+1)} &= \frac{m_p}{\gamma_p n_p + \lambda_{p-1} m_p}\big(-d\varepsilon_{p-1,p-1}^{(k)} + \lambda_{p-1}\varepsilon_{p-1,p-1}^{(k)}\big), \end{aligned}$$

where

$$d_i = \left(\gamma_i^2 + \lambda_i\lambda_{i-1}\right)m_i + \gamma_i(\lambda_i + \lambda_{i-1})n_i, \quad i = 2, \ldots, p-1,$$
$$n_i = e^{\gamma_i \ell_i} - e^{-\gamma_i \ell_i} \quad \text{and} \quad m_i = e^{\gamma_i \ell_i} + e^{-\gamma_i \ell_i}, \quad i = 1, \ldots, p.$$

By differentiating equations (6)–(8) we obtain expressions similar to the above that relate $d\varepsilon_{1,1}^{(k+1)}$, $d\varepsilon_{i,i-1}^{(k+1)}$, $d\varepsilon_{i,i}^{(k+1)}$, $i = 2, \ldots, p-1$, and $d\varepsilon_{p,p-1}^{(k+1)}$ with associated values from the iteration (k); these are

$$\begin{aligned}
d\varepsilon_{1,1}^{(k+1)} &= \frac{\gamma_1 n_1}{\gamma_1 n_1 + \lambda_1 m_1}\left(d\varepsilon_{2,1}^{(k)} + \lambda_1 \varepsilon_{2,1}^{(k)}\right),\\
d\varepsilon_{i,i-1}^{(k+1)} &= \frac{\gamma_i}{d_i}\left[(\gamma_i m_i + \lambda_i n_i)\left(d\varepsilon_{i-1,i-1}^{(k)} - \lambda_{i-1}\varepsilon_{i-1,i-1}^{(k)}\right) + 2\lambda_{i-1}\left(d\varepsilon_{i+1,i}^{(k)} + \lambda_i \varepsilon_{i+1,i}^{(k)}\right)\right],\\
d\varepsilon_{i,i}^{(k+1)} &= \frac{\gamma_i}{d_i}\left[(\gamma_i m_i + \lambda_{i-1} n_i)\left(d\varepsilon_{i+1,i}^{(k)} + \lambda_i \varepsilon_{i+1,i}^{(k)}\right) + 2\lambda_i\left(d\varepsilon_{i-1,i-1}^{(k)} - \lambda_{i-1}\varepsilon_{i-1,i-1}^{(k)}\right)\right],\\
d\varepsilon_{p,p-1}^{(k+1)} &= \frac{\gamma_p n_p}{\gamma_p n_p + \lambda_{p-1} m_p}\left(d\varepsilon_{p-1,p-1}^{(k)} - \lambda_{p-1}\varepsilon_{p-1,p-1}^{(k)}\right).
\end{aligned}$$

Now we order the errors on the interface points to create a sequence of error vectors as follows, for $k = 0, 1, 2, \ldots,$

$$\begin{aligned}
\underline{\varepsilon}^{(k)} \equiv \big[&d\varepsilon_{1,1}^{(k)}, \varepsilon_{1,1}^{(k)}, \varepsilon_{2,1}^{(k)}, d\varepsilon_{2,1}^{(k)}, d\varepsilon_{2,2}^{(k)}, \varepsilon_{2,2}^{(k)}, \varepsilon_{3,2}^{(k)}, d\varepsilon_{3,2}^{(k)}, \ldots,\\
&d\varepsilon_{i,i}^{(k)}, \varepsilon_{i,i}^{(k)}, \varepsilon_{i+1,i}^{(k)}, d\varepsilon_{i+1,i}^{(k)}, \ldots, d\varepsilon_{p-1,p-1}^{(k)}, \varepsilon_{p-1,p-1}^{(k)}, \varepsilon_{p,p-1}^{(k)}, d\varepsilon_{p,p-1}^{(k)}\big]^{\mathrm{T}}.
\end{aligned}$$

We obtain the following relation between the vectors of interface errors in the two consecutive iteration steps (k) and $(k+1)$

$$\underline{\varepsilon}^{(k+1)} = M\underline{\varepsilon}^{(k)}, \quad k = 0, 1, \ldots, \tag{9}$$

where the iteration matrix $M \in \mathbb{R}^{4(p-1)\times 4(p-1)}$ has the form

$$M = \begin{bmatrix}
0 & M_{1,2} & 0 & 0 & 0 & 0 & \cdots & 0\\
M_{2,1} & 0 & 0 & M_{2,4} & 0 & 0 & \cdots & 0\\
M_{3,1} & 0 & 0 & M_{3,4} & 0 & 0 & \cdots & 0\\
0 & 0 & M_{4,3} & 0 & 0 & M_{4,6} & \cdots & 0\\
0 & 0 & M_{5,3} & 0 & 0 & M_{5,6} & \cdots & 0\\
\vdots & \vdots & & \ddots & \ddots & \ddots & & \vdots\\
0 & 0 & \cdots & 0 & M_{2(p-1)-2,2(p-1)-3} & 0 & 0 & M_{2(p-1)-2,2(p-1)}\\
0 & 0 & \cdots & 0 & M_{2(p-1)-1,2(p-1)-3} & 0 & 0 & M_{2(p-1)-1,2(p-1)}\\
0 & 0 & \cdots & 0 & 0 & 0 & M_{2(p-1),2(p-1)-1} & 0
\end{bmatrix}. \tag{10}$$

The submatrices of M are as follows:

$$M_{1,2} = \frac{1}{\gamma_1 n_1 + \lambda_1 m_1}\begin{bmatrix} \gamma_1 n_1 \lambda_1 & \gamma_1 n_1 \\ m_1\lambda_1 & m_1 \end{bmatrix},$$

for $i = 2, \ldots, p-1$,

$$M_{2(i-1),2(i-1)-1} = \frac{1}{d_i}\begin{bmatrix} -(\gamma_i n_i + \lambda_i m_i) & \lambda_{i-1}(\gamma_i n_i + \lambda_i m_i) \\ \gamma_i(\gamma_i m_i + \lambda_i n_i) & -\gamma_i\lambda_{i-1}(\gamma_i m_i + \lambda_i n_i) \end{bmatrix},$$

$$M_{2(i-1)+1,2(i-1)+2} = \frac{1}{d_i}\begin{bmatrix} \gamma_i\lambda_i(\gamma_i m_i + \lambda_{i-1} n_i) & \gamma_i(\gamma_i m_i + \lambda_{i-1} n_i) \\ \lambda_i(\gamma_i n_i + \lambda_{i-1} m_i) & (\gamma_i n_i + \lambda_{i-1} m_i) \end{bmatrix},$$

$$M_{2(i-1),2(i-1)+2} = \frac{2\gamma_i}{d_i}\begin{bmatrix} \lambda_i & 1 \\ \lambda_i\lambda_{i-1} & \lambda_{i-1} \end{bmatrix}, \qquad M_{2(i-1)+1,2(i-1)-1} = \frac{2\gamma_i}{d_i}\begin{bmatrix} \lambda_i & -\lambda_i\lambda_{i-1} \\ -1 & \lambda_{i-1} \end{bmatrix},$$

and

$$M_{2(p-1),2(p-1)-1} = \frac{1}{\gamma_p n_p + \lambda_{p-1} m_p}\begin{bmatrix} -m_p & \lambda_{p-1} m_p \\ \gamma_p n_p & -\gamma_p n_p \lambda_{p-1} \end{bmatrix}.$$

For the rest of the analysis in this section we use a methodology similar to the one found in [9]. In the following lemma we construct a matrix $\widetilde{M} \in \mathbb{R}^{2(p-1)\times 2(p-1)}$ of reduced size which is spectrally equivalent to the iteration matrix M and whose special non-zero structure lets us select optimum values for the relaxation parameters λ_i.

Lemma 2. *The two matrices M and $\widetilde{M}$ have the same non-zero eigenvalues, i.e.,*

$$\sigma(M)\backslash\{0\} = \sigma\big(\widetilde{M}\big)\backslash\{0\}, \tag{11}$$

where

$$\widetilde{M} = \begin{bmatrix} 0 & \widetilde{M}_{1,2} & 0 & 0 & 0 & 0 & \cdots & 0 \\ \widetilde{M}_{2,1} & 0 & 0 & \widetilde{M}_{2,4} & 0 & 0 & \cdots & 0 \\ \widetilde{M}_{3,1} & 0 & 0 & \widetilde{M}_{3,4} & 0 & 0 & \cdots & 0 \\ 0 & 0 & \widetilde{M}_{4,3} & 0 & 0 & \widetilde{M}_{4,6} & \cdots & 0 \\ 0 & 0 & \widetilde{M}_{5,3} & 0 & 0 & \widetilde{M}_{5,6} & \cdots & 0 \\ \vdots & \vdots & & \ddots & \ddots & \ddots & & \vdots \\ 0 & 0 & \cdots & 0 & \widetilde{M}_{2(p-1)-2,2(p-1)-3} & 0 & 0 & \widetilde{M}_{2(p-1)-2,2(p-1)} \\ 0 & 0 & \cdots & 0 & \widetilde{M}_{2(p-1)-1,2(p-1)-3} & 0 & 0 & \widetilde{M}_{2(p-1)-1,2(p-1)} \\ 0 & 0 & \cdots & 0 & 0 & 0 & \widetilde{M}_{2(p-1),2(p-1)-1} & 0 \end{bmatrix}. \tag{12}$$

The elements of $\widetilde{M}$ are defined as follows:

$$\widetilde{M}_{1,2} = \frac{-\gamma_1 n_1 + \lambda_1 m_1}{\gamma_1 n_1 + \lambda_1 m_1},$$

for $i = 2, \ldots, p-1$,

$$\widetilde{M}_{2(i-1),2(i-1)-1} = \frac{\lambda_{i-1}(\gamma_i n_i + \lambda_i m_i) - \gamma_i(\gamma_i m_i + \lambda_i n_i)}{d_i},$$

$$\widetilde{M}_{2(i-1)+1,2(i-1)+2} = \frac{\lambda_i(\gamma_i n_i + \lambda_{i-1} m_i) - \gamma_i(\gamma_i m_i + \lambda_{i-1} n_i)}{d_i},$$

$$\widetilde{M}_{2(i-1),2(i-1)+2} = \frac{4\gamma_i\lambda_{i-1}}{d_i}, \qquad \widetilde{M}_{2(i-1)+1,2(i-1)-1} = \frac{4\gamma_i\lambda_i}{d_i},$$

and

$$\widetilde{M}_{2(p-1),2(p-1)-1} = \frac{-\gamma_p n_p + \lambda_{p-1} m_p}{\gamma_p n_p + \lambda_{p-1} m_p}.$$

Proof. We define the non-singular matrix

$$Q = \operatorname{diag}\big(Q_1, Q_1^{\mathrm{T}}, Q_2, Q_2^{\mathrm{T}}, \ldots, Q_{p-1}, Q_{p-1}^{\mathrm{T}}\big),$$

where

$$Q_i = Q_i^{-1} = \begin{bmatrix} 1 & -\lambda_i \\ 0 & -1 \end{bmatrix}, \quad Q_i^{\mathrm{T}} = Q_i^{-\mathrm{T}} = \begin{bmatrix} 1 & 0 \\ -\lambda_i & -1 \end{bmatrix}, \quad i = 1, \ldots, p-1,$$

and consider the similarity transformation matrix $Q^{-1}MQ$ whose submatrices are specified by the following relations:

$$Q_1^{-1} M_{1,2} Q_1^{\mathrm{T}} = \begin{bmatrix} 0 & \dfrac{-\gamma_1 n_1 + \lambda_1 m_1}{\gamma_1 n_1 + \lambda_1 m_1} \\ 0 & \dfrac{m_1}{\gamma_1 n_1 + \lambda_1 m_1} \end{bmatrix},$$

for $i = 2, \ldots, p-1$,

$$Q_{i-1}^{-\mathrm{T}} M_{2(i-1),2(i-1)-1} Q_{i-1} = \frac{1}{d_i} \begin{bmatrix} -(\gamma_i n_i + \lambda_i m_i) & 0 \\ \lambda_{i-1}(\gamma_i n_i + \lambda_i m_i) - \gamma_i(\gamma_i m_i + \lambda_i n_i) & 0 \end{bmatrix},$$

$$Q_{i-1}^{-\mathrm{T}} M_{2(i-1),2(i-1)+2} Q_i^{\mathrm{T}} = \frac{2\gamma_i}{d_i} \begin{bmatrix} 0 & -1 \\ 0 & 2\lambda_{i-1} \end{bmatrix},$$

$$Q_i^{-1} M_{2(i-1)+1,2(i-1)-1} Q_{i-1} = \frac{2\gamma_i}{d_i} \begin{bmatrix} 2\lambda_i & 0 \\ 1 & 0 \end{bmatrix},$$

$$Q_i^{-1} M_{2(i-1)+1,2(i-1)+2} Q_i^{\mathrm{T}} = \frac{1}{d_i} \begin{bmatrix} 0 & -\gamma_i(\gamma_i m_i + \lambda_{i-1} n_i) + \lambda_i(\gamma_i n_i + \lambda_{i-1} m_i) \\ 0 & \gamma_i p_i + \lambda_{i-1} m_i \end{bmatrix},$$

and

$$Q_{p-1}^{-\mathrm{T}} M_{2(p-1),2(p-1)-1} Q_{p-1} = \frac{1}{\gamma_p n_p + \lambda_{p-1} m_p} \begin{bmatrix} -m_p & 0 \\ m_p \lambda_{p-1} - \gamma_p n_p & 0 \end{bmatrix}.$$

A simple comparison of the above relations with the elements of the matrix $\widetilde{M}$ and the fact that there exists (Lemma 3.2 in [9]) a permutation matrix P such that

$$P^{\mathrm{T}} Q^{\mathrm{T}} M Q P = \begin{bmatrix} 0 & * \\ 0 & \widetilde{M} \end{bmatrix},$$

complete the proof of the lemma. □

We conclude this section with the main theorem that presents analytic expressions for the optimum relaxation parameters.

Theorem 3. *Consider the model problem* (1) *and a non-overlapping decomposition of Ω into p subdomains Ω_i of length ℓ_i, $i = 1, \ldots, p$. If the parameters λ_i involved in the **ROB** interface relaxation method are selected as*

$$\lambda_{p-1} = \frac{\gamma_p n_p}{m_p}, \qquad \lambda_{i-1} = \frac{\gamma_i(\gamma_i m_i + \lambda_i n_i)}{\gamma_i n_i + \lambda_i m_i}, \quad i = p-1, \ldots, 2, \tag{13}$$

then the spectral radius of the iteration matrix M is zero.

Proof. It can been seen (Lemma 3.2 in [9]) that if we set $\widetilde{M}_{2(i-1),2(i-1)-1} = 0,\ i = 2,\ldots,p$, then we obtain that $\sigma(\widetilde{M}) = 0$. This leads to the following equations.

$$\lambda_{p-1} m_p - \gamma_p n_p = 0$$

and

$$\lambda_{i-1}(\gamma_i n_i + \lambda_i m_i) - \gamma_i(\gamma_i m_i + \lambda_i n_i) = 0, \quad i = 2,\ldots,p-1. \tag{14}$$

To conclude the proof, we back solve for $\lambda_i,\ i = p-1,\ldots,1$ and use the previous lemma. □

3.2. *"Optimum" relaxation parameters for the **AVE** method*

Using the notation adopted in the previous section and the **AVE** algorithm given in Section 2 we easily see that the error functions involved satisfy the following differential equations: For the odd steps the equation for the first subdomain is

$$\begin{aligned} &L_1 \varepsilon_1^{(2k+1)}(x) = 0, \quad x \in \Omega_1, \\ &\varepsilon_{1,0}^{(2k+1)} = 0, \qquad d\varepsilon_{1,1}^{(2k+1)} = \beta_1 d\varepsilon_{1,1}^{(2k)} + (1-\beta_1) d\varepsilon_{2,1}^{(2k)}, \end{aligned} \tag{15}$$

for the ith interior subdomain, $i = 2,\ldots,p-1$, the equation is

$$\begin{aligned} &L_i \varepsilon_i^{(2k+1)}(x) = 0, \quad x \in \Omega_i, \\ &d\varepsilon_{i,i-1}^{(2k+1)} = \beta_{i-1} d\varepsilon_{i-1,i-1}^{(2k)} + (1-\beta_{i-1}) d\varepsilon_{i,i-1}^{(2k)}, \\ &d\varepsilon_{i,i}^{(2k+1)} = \beta_i d\varepsilon_{i,i}^{(2k)} + (1-\beta_i) d\varepsilon_{i+1,i}^{(2k)}, \end{aligned} \tag{16}$$

and for the last subdomain the equation is

$$\begin{aligned} &L_p \varepsilon_p^{(2k+1)}(x) = 0, \quad x \in \Omega_p, \\ &d\varepsilon_{p,p-1}^{(2k+1)} = \beta_{p-1} d\varepsilon_{p-1,p-1}^{(2k)} + (1-\beta_{p-1}) d\varepsilon_{p,p-1}^{(2k)}, \\ &\varepsilon_{p,p}^{(2k+1)} = 0. \end{aligned} \tag{17}$$

For the even steps the equation for the first subdomain is

$$\begin{aligned} &L_1 \varepsilon_1^{(2k+2)}(x) = 0, \quad x \in \Omega_1, \\ &\varepsilon_{1,0}^{(2k+2)} = 0, \qquad \varepsilon_{1,1}^{(2k+2)} = \alpha_1 \varepsilon_{1,1}^{(2k+1)} + (1-\alpha_1) \varepsilon_{2,1}^{(2k+1)}, \end{aligned} \tag{18}$$

for the ith interior subdomain, $i = 2,\ldots,p-1$, the equation is

$$\begin{aligned} &L_i \varepsilon_i^{(2k+2)}(x) = 0, \quad x \in \Omega_i, \\ &\varepsilon_{i,i-1}^{(2k+2)} = \alpha_{i-1} \varepsilon_{i-1,i-1}^{(2k+1)} + (1-\alpha_{i-1}) \varepsilon_{i,i-1}^{(2k+1)}, \\ &\varepsilon_{i,i}^{(2k+2)} = \alpha_i \varepsilon_{i,i}^{(2k+1)} + (1-\alpha_i) \varepsilon_{i+1,i}^{(2k+1)}, \end{aligned} \tag{19}$$

and for the last subdomain the equation is

$$\begin{aligned} &L_p \varepsilon_p^{(2k+2)}(x) = 0, \quad x \in \Omega_p, \\ &\varepsilon_{p,p-1}^{(2k+2)} = \alpha_{p-1} \varepsilon_{p-1,p-1}^{(2k+1)} + (1-\alpha_{p-1}) \varepsilon_{p,p-1}^{(2k+1)}, \qquad \varepsilon_{p,p}^{(2k+2)} = 0. \end{aligned} \tag{20}$$

The solutions to the Neumann problems (15)–(17) are given by (see Lemma 1)

$$\varepsilon_1^{(2k+1)}(x) = \frac{1}{\gamma_1 m_1}\big(e^{\gamma_1(x-x_0)} - e^{-\gamma_1(x-x_0)}\big)\big(\beta_1 d\varepsilon_{1,1}^{(2k)} + (1-\beta_1)d\varepsilon_{2,1}^{(2k)}\big),$$

$$\begin{aligned}\varepsilon_i^{(2k+1)}(x) = \frac{1}{\gamma_i n_i}\Big\{&\big(-e^{\gamma_i(x_i-x)} - e^{-\gamma_i(x_i-x)}\big)\big(\beta_{i-1} d\varepsilon_{i-1,i-1}^{(2k)} + (1-\beta_{i-1})d\varepsilon_{i,i-1}^{(2k)}\big)\\ &+\big(e^{\gamma_i(x-x_{i-1})} + e^{-\gamma_i(x-x_{i-1})}\big)\big(\beta_i d\varepsilon_{i,i}^{(2k)} + (1-\beta_i)d\varepsilon_{i+1,i}^{(2k)}\big)\Big\}, \quad i = 2,\dots,p-1,\end{aligned}$$

$$\varepsilon_p^{(2k+1)}(x) = \frac{1}{\gamma_p m_p}\big(-e^{\gamma_p(x_p-x)} + e^{-\gamma_p(x_p-x)}\big)\big(\beta_{p-1} d\varepsilon_{p-1,p-1}^{(2k)} + (1-\beta_{p-1})d\varepsilon_{p,p-1}^{(2k)}\big).$$

The solutions to the Dirichlet problems (18)–(20) are given by

$$\varepsilon_1^{(2k+2)}(x) = \frac{1}{n_i}\big(e^{\gamma_1(x-x_0)} - e^{-\gamma_1(x-x_0)}\big)\big(\alpha_1 \varepsilon_{1,1}^{(2k+1)} + (1-\alpha_1)\varepsilon_{2,1}^{(2k+1)}\big),$$

$$\begin{aligned}\varepsilon_i^{(2k+2)}(x) = \frac{1}{n_i}\Big\{&\big(e^{\gamma_i(x_i-x)} - e^{-\gamma_i(x_i-x)}\big)\big(\alpha_{i-1}\varepsilon_{i-1,i-1}^{(2k+1)} + (1-\alpha_{i-1})\varepsilon_{i,i-1}^{(2k+1)}\big)\\ &+\big(e^{\gamma_i(x-x_{i-1})} - e^{-\gamma_i(x-x_{i-1})}\big)\big(\alpha_i \varepsilon_{i,i}^{(2k+1)} + (1-\alpha_i)\varepsilon_{i+1,i}^{(2k+1)}\big)\Big\}, \quad i = 2,\dots,p-1,\end{aligned}$$

$$\varepsilon_p^{(2k+2)}(x) = \frac{1}{n_p}\big(e^{\gamma_p(x_p-x)} - e^{-\gamma_p(x_p-x)}\big)\big(\alpha_{p-1}\varepsilon_{p-1,p-1}^{(2k+1)} + (1-\alpha_{p-1})\varepsilon_{p,p-1}^{(2k+1)}\big).$$

If, for $k = 0, 1, \dots$, we define the vectors

$$\underline{\varepsilon}^{(k)} \equiv \big[\varepsilon_{1,1}^{(k)}, \varepsilon_{2,2}^{(k)}, \dots, \varepsilon_{p-1,p-1}^{(k)}\big]^{\mathrm{T}} \quad \text{and} \quad \underline{d\varepsilon}^{(k)} \equiv \big[d\varepsilon_{1,1}^{(k)}, d\varepsilon_{2,2}^{(k)}, \dots, d\varepsilon_{p-1,p-1}^{(k)}\big]^{\mathrm{T}} \tag{21}$$

then we get from the above that

$$\underline{\varepsilon}^{(2k+2)} = M^D \underline{d\varepsilon}^{(2k+1)}, \tag{22}$$

$$\underline{d\varepsilon}^{(2k+1)} = M^N \underline{\varepsilon}^{(2k)}, \tag{23}$$

where the Dirichlet and Neumann iteration matrices $M^D, M^N \in \mathbb{R}^{(p-1)\times(p-1)}$ are tridiagonal with elements

$$\begin{aligned}
&M_{1,1}^D = \frac{\alpha_1 m_1}{n_1\gamma_1} - \frac{(1-\alpha_1)n_2}{m_2\gamma_2}, && M_{p-1,p-1}^D = \frac{\alpha_{p-1}n_{p-1}}{m_{p-1}\gamma_{p-1}} - \frac{(1-\alpha_{p-1})m_p}{n_p\gamma_p},\\
&M_{i,i}^D = \frac{\alpha_i n_i}{m_i\gamma_i} - \frac{(1-\alpha_i)n_{i+1}}{m_{i+1}\gamma_{i+1}}, && i = 2,\dots,p-2,\\
&M_{i,i+1}^D = \frac{2(1-\alpha_i)}{m_{i+1}\gamma_{i+1}}, && i = 2,\dots,p-1,\\
&M_{i+1,i}^D = -\frac{2\alpha_i}{m_i\gamma_i}, && i = 1,\dots,p-2,
\end{aligned} \tag{24}$$

$$
\begin{aligned}
&M^N_{1,1} = \frac{\beta_1 n_1 \gamma_1}{m_1} - \frac{(1-\beta_1) n_2 \gamma_2}{m_2}, \qquad M^N_{p-1,p-1} = \frac{\beta_{p-1} n_{p-1} \gamma_{p-1}}{m_{p-1}} - \frac{(1-\beta_{p-1}) n_p \gamma_p}{m_p},\\
&M^N_{i,i} = \frac{\beta_i n_i \gamma_i}{m_i} - \frac{(1-\beta_i) n_{i+1} \gamma_{i+1}}{m_{i+1}}, \quad i = 2, \ldots, p-2,\\
&M^N_{i,i+1} = \frac{2(1-\beta_i)\gamma_{i+1}}{m_{i+1}}, \qquad i = 2, \ldots, p-1,\\
&M^N_{i+1,i} = -\frac{2\beta_i \gamma_i}{m_i}, \qquad i = 1, \ldots, p-2.
\end{aligned} \tag{25}
$$

For $p = 2$ it is easy to see (force the roots of the characteristic polynomial of M^D or M^N to be zero) that $\alpha_1 = \frac{m_2 n_1 \gamma_1}{m_2 n_1 \gamma_1 + m_1 n_2 \gamma_2}$ or $\beta_1 = \frac{m_1 n_2 \gamma_2}{m_1 n_2 \gamma_2 + m_2 n_1 \gamma_1}$ are optimum values and achieve immediate convergence. For $p > 2$ we have been unable to derive optimum values for the relaxation parameters. Instead we obtain values for them that are optimum in the max-norm (see Appendix A).

Theorem 4. *Consider the iteration matrix $M \equiv M^N M^D$ of the **AVE** method associated with the model problem* (1) *and a non-overlapping decomposition of Ω into p subdomains Ω_i of length ℓ_i, $i = 1, \ldots, p$ with $\gamma_i = \gamma$ in $i = 1, \ldots, p$. For the values the relaxation parameters given below, the max-norms of M^N and M^D are minimized and the matrix M is a contraction mapping, with respect to the max-norm*:

$$\alpha_1 = \frac{n_1 n_2}{n_1 n_2 + m_1 m_2}, \qquad \alpha_{p-1} = \frac{m_p m_{p-1}}{m_p m_{p-1} + n_p n_{p-1}}, \tag{26}$$

$$\alpha_i = \frac{m_i n_{i+1}}{m_i n_{i+1} + m_{i+1} n_i}, \quad i = 2, \ldots, p-2 \tag{27}$$

and

$$\beta_1 = \frac{m_1 n_2}{m_1 n_2 + m_2 n_1}, \qquad \beta_{p-1} = \frac{m_{p-1} n_p}{m_{p-1} n_p + m_p n_{p-1}}, \tag{28}$$

$$\beta_i = \frac{m_i n_{i+1}}{m_i n_{i+1} + m_{i+1} n_i}, \quad i = 2, \ldots, p-2, \tag{29}$$

provided that $\ell_i > \frac{\ln(1+\sqrt{2})}{\gamma}$, $i = 1, \ldots, p$.

Proof. To minimize the max-norm of the iteration matrix, it is sufficient to minimize the quantity

$$
\begin{aligned}
&f(\alpha_i, \beta_i, \beta_{i-1}, \beta_{i+1})\\
&\quad = 4\frac{\alpha_i \beta_{i-1}}{m_i m_{i-1}} + \frac{2}{m_i}\left|\alpha_i \frac{\beta_{i-1}(m_i n_{i-1} + m_{i-1} n_i) - m_{i-1} n_i}{m_{i-1} m_i} + \beta_i \frac{\alpha_i (m_{i+1} n_i + m_i n_{i+1}) - m_i n_{i+1}}{m_i m_{i+1}}\right|\\
&\qquad + \left|-4\frac{\alpha_i(1-\beta_{i-1})}{m_i^2} + \frac{\alpha_i (m_{i+1} n_i + m_i n_{i+1}) - m_i n_{i+1}}{m_i m_{i+1}} \frac{\beta_i (m_{i+1} n_i + m_i n_{i+1}) - m_i n_{i+1}}{m_i m_{i+1}}\right.\\
&\qquad\quad \left. - 4\frac{(1-\alpha_i)\beta_{i+1}}{m_{i+1}^2}\right|\\
&\qquad + \frac{2}{m_{i+1}}\left|\frac{\alpha_i (m_{i+1} n_i + m_i n_{i+1}) - m_i n_{i+1}}{m_i m_{i+1}}(1-\beta_i)\right.\\
&\qquad\quad \left. + \frac{\beta_{i+1}(m_{i+2} n_{i+1} + m_{i+1} n_{i+2}) - m_{i+1} n_{i+2}}{m_{i+1} m_{i+2}}(1-\alpha_i)\right| + 4\frac{(1-\alpha_i)(1-\beta_{i+1})}{m_i m_{i+1}}.
\end{aligned} \tag{30}
$$

One can determine values for $\alpha_i, \beta_i, \beta_{i-1}$ and β_{i+1} that minimize f by an elementary but very lengthy and tedious analysis which involves splitting the absolute values and considering several different cases. (This analysis is presented in Appendix A.) Here, instead, we give an indication why this theorem is true.

Set

$$\alpha_i = \alpha_i^* \equiv \frac{m_i n_{i+1}}{m_{i+1}n_i + m_i n_{i+1}}, \qquad \beta_i = \beta_i^* \equiv \frac{m_i n_{i+1}}{m_{i+1}n_i + m_i n_{i+1}},$$

$$\beta_{i-1} = \beta_{i-1}^* \equiv \frac{m_{i-1} n_i}{m_{i-1}n_i + m_i n_{i-1}} \quad \text{and} \quad \beta_{i+1} = \beta_{i+1}^* \equiv \frac{m_{i+1} n_{i+2}}{m_{i+1}n_{i+2} + m_{i+2} n_{i+1}}.$$

Then the expressions in the absolute values of (30) become zero and so we have

$$f\left(\alpha_i^*, \beta_i^*, \beta_{i-1}^*, \beta_{i+1}^*\right) = \frac{4}{m_{i+1}n_i + m_i n_{i+1}} \left(\frac{m_{i+1}(m_i + m_{i-1})}{m_{i-1}n_i + m_i n_{i-1}} + \frac{m_i (m_{i+1} + m_{i+2})}{m_{i+1}n_{i+2} + m_{i+2} n_{i+1}} \right).$$

Under the constraint that $\ell_j > \frac{\ln(1+\sqrt{2})}{\gamma}$ we have that $n_j > 2,\ j = i-1, i, i+1$, and therefore we have

$$f\left(\alpha_i^*, \beta_i^*, \beta_{i-1}^*, \beta_{i+1}^*\right) < \frac{4}{2(m_i + m_{i+1})} \left(\frac{m_{i+1}(m_i + m_{i-1})}{2(m_i + m_{i-1})} + \frac{m_i (m_{i+1} + m_{i+2})}{2(m_{i+2} + m_{i+1})} \right) = 1.$$

Continuing in the same way for the 1st, 2nd, $(p-2)$th and $(p-1)$th rows of the iteration matrix, we get optimum values for the relaxation parameters for all the interface points. □

4. Numerical experiments

The purpose of the numerical experiments performed in this study is two-fold. First to verify and elucidate our theoretically determined relaxation parameter values on a class of one-dimensional problems and second to examine how effective these parameters values are for two-dimensional PDEs. All experiments reported here are performed in single precision on SUN workstations.

4.1. One-dimensional case

We have implemented the two IR methods considered in this paper using MATLAB. All MATLAB files we use to produce the one-dimensional data in this section are available through our web page.[2] Implementations of several other relaxation schemes also can be found there. We use zero as initial guess and consider the following model problem:

$$Lu \equiv -u''(x) + \gamma^2 u(x) = f(x), \quad x \in (0,1),\ u(0) = 0,\ u(1) = 0, \tag{31}$$

where the right hand side function f is selected such that the true solution $u(x)$ is either

DP1 $u(x) = \cosh(2x-1) - \cosh(1.0)$, or
DP2 $u(x) = e^{x+4}x(x-1)(x-0.7)$.

[2] http://www.cs.purdue.edu/homes/giwta/dom-dec/1_dim/matlab/index.html.

Table 1
The max-norm of the error and the computed values of the convergence factor of the **ROB** method applied to model problem (31)-DP1 ($\gamma^2 = 2$). In the first column we have the iteration number, in the first row the discretization step-size and in the second row the number of equal subdomains

Iter	$h = 0.01$				$h = 0.005$			
	$p = 2$	$p = 4$	$p = 10$	$p = 20$	$p = 2$	$p = 4$	$p = 10$	$p = 20$
2	3.08E−5	1.48E−1	2.74E−1	3.87E−1	7.83E−6	1.48E−1	2.74E−1	3.87E−1
	(0.2966)	(0.2997)	(0.2424)	(0.1811)	(0.2966)	(0.2992)	(0.2421)	(0.1809)
3	1.19E−5	7.18E−2	1.72E−1	3.00E−1	3.07E−6	7.18E−2	1.72E−1	3.00E−1
	(0.4447)	(0.4635)	(0.4409)	(0.3723)	(0.4447)	(0.4635)	(0.4408)	(0.3721)
4	1.19E−5	3.18E−2	1.42E−1	2.27E−1	3.07E−6	3.18E−2	1.42E−1	2.27E−1
	(0.5446)	(0.5524)	(0.5651)	(0.5106)	(0.5446)	(0.5524)	(0.5651)	(0.5105)
5	1.19E−5	1.41E−2	1.53E−1	1.75E−1	3.07E−6	1.41E−2	1.53E−1	1.75E−1
	(0.6150)	(0.6167)	(0.6425)	(0.6063)	(0.6150)	(0.6166)	(0.6425)	(0.6063)
8	1.19E−5	6.11E−5	7.25E−2	1.64E−1	3.07E−6	1.52E−5	7.24E−2	1.64E−1
	(0.7379)	(0.7379)	(0.7494)	(0.7576)	(0.7379)	(0.7379)	(0.7494)	(0.7576)
16	1.19E−5	6.14E−5	2.04E−3	7.43E−2	3.07E−6	1.52E−5	2.05E−3	7.41E−2
	(0.8590)	(0.8590)	(0.8590)	(0.8658)	(0.8590)	(0.8590)	(0.8590)	(0.8658)
20	1.19E−5	6.14E−5	2.13E−4	3.99E−2	3.07E−6	1.52E−5	5.28E−5	3.98E−2
	(0.8855)	(0.8855)	(0.8855)	(0.8883)	(0.8855)	(0.8855)	(0.8855)	(0.8883)
32	1.19E−5	6.14E−5	2.14E−4	2.23E−3	3.07E−6	1.52E−5	5.32E−5	2.18E−3
	(0.9268)	(0.9268)	(0.9268)	(0.9268)	(0.9268)	(0.9268)	(0.9268)	(0.9268)
36	1.19E−5	6.14E−5	2.14E−4	4.72E−4	3.07E−6	1.52E−5	5.32E−5	2.54E−4
	(0.9347)	(0.9347)	(0.9347)	(0.9347)	(0.9347)	(0.9347)	(0.9347)	(0.9347)

In Table 1 we present the max norm of the error $\|u^{(k)} - u\|_\infty$ and the computed convergence factor

$$r_k = \sqrt[k]{\left\|Lu^{(k)} - f\right\|_\infty / \left\|Lu^{(0)} - f\right\|_\infty}, \quad k = 1, 2, \ldots$$

of the **ROB** method applied to the model problem (31) with $\gamma^2 = 2$ and solution DP1. We assume that the domain is decomposed into $p = 2, 4, 10, 20$ domains of equal size. We use the 5-point star difference approximation with two different global discretization steps $h = 0.01$ and $h = 0.005$ to solve the DE. Similarly in Table 2 we consider the **AVE** method and set $\gamma^2 = 10$. The rapid rate of convergence is easily observed as one moves down along any column. Note that this convergence is not immediate (1 iteration) as our theory might indicate. It can be shown [22] that this is mainly due to the particular block structure of the Jordan form of the iteration matrices which may require from 1 to $2(p-1)$ iteration steps instead of one.

It can be also observed that, as the computed convergence factors indicate, the rate of convergence of both methods does not seem to depend on the fineness of the domain discretization. Nevertheless, the order h^2 finite difference discretization convergence rate is preserved. The rate of convergence does depend, as expected, on both the number of subdomains and the coefficient γ^2. Extensive numerical experiments (some of them presented in Fig. 3 below, and some others that are not included in this paper) show that the rate of convergence increases as γ^2 increases for both methods but much more rapidly in

Table 2
The max norm of the error and the computed values of the convergence factor of the **AVE** method applied to model problem (31)-DP1 ($\gamma^2 = 10$). In the first column we have the iteration number, in the first row the discretization step-size and in the second row the number of equal subdomains

Iter	$h = 0.01$				$h = 0.005$			
	$p = 2$	$p = 4$	$p = 10$	$p = 20$	$p = 2$	$p = 4$	$p = 10$	$p = 20$
2	1.39E−6 (0.0965)	2.32E−4 (0.0965)	1.43E−2 (0.0966)	1.03E−1 (0.0966)	3.48E−7 (0.0965)	2.34E−4 (0.0965)	1.43E−2 (0.0966)	1.04E−1 (0.0966)
3	1.39E−6 (0.2103)	5.23E−6 (0.2104)	7.18E−3 (0.2097)	2.23E−1 (0.2104)	3.48E−7 (0.2103)	3.71E−6 (0.2104)	7.23E−3 (0.2097)	2.25E−1 (0.2104)
4	1.39E−6 (0.3106)	1.99E−6 (0.3106)	4.58E−3 (0.3113)	5.39E−1 (0.3419)	3.48E−7 (0.3106)	4.65E−7 (0.3106)	4.62E−3 (0.3113)	5.44E−1 (0.3423)
5	1.39E−6 (0.3924)	2.04E−6 (0.3924)	3.15E−3 (0.3920)	1.41E+0 (0.4934)	3.48E−7 (0.3924)	5.10E−7 (0.3924)	3.19E−3 (0.3920)	1.43E+0 (0.4945)
8	1.39E−6 (0.5573)	2.04E−6 (0.5573)	8.61E−4 (0.5574)	4.22E+1 (0.9617)	3.48E−7 (0.5573)	5.09E−7 (0.5573)	8.76E−4 (0.5574)	4.32E+1 (0.9644)
16	1.39E−6 (0.7465)	2.04E−6 (0.7465)	2.93E−5 (0.7465)	5.18E+5 (1.830)	3.48E−7 (0.7465)	5.09E−7 (0.7465)	2.65E−5 (0.7465)	5.43E+5 (1.770)
20	1.39E−6 (0.7915)	2.04E−6 (0.7915)	9.18E−6 (0.7915)	1.68E+6 (1.993)	3.48E−7 (0.7915)	5.09E−7 (0.7915)	5.58E−6 (0.7915)	6.19E+7 (2.001)
32	1.39E−6 (0.8640)	2.04E−6 (0.8640)	7.44E−6 (0.8640)	2.68E+14 (2.487)	3.48E−7 (0.8640)	5.09E−7 (0.8640)	1.86E−6 (0.8640)	2.95E+14 (2.491)
36	1.39E−6 (0.8781)	2.04E−6 (0.8781)	7.44E−6 (0.8812)	4.41E+16 (2.586)	3.48E−7 (0.8781)	5.09E−7 (0.8781)	1.86E−6 (0.8749)	6.29E+16 (2.597)

the **AVE** case. The **AVE** method diverges for $\gamma^2 = 10$ and $p = 20$. This is in good agreement with the restriction

$$\ell_i > \frac{\ln(1+\sqrt{2})}{\gamma}, \quad i = 1, \ldots, p,$$

imposed by Theorem 4. This restriction seems to be necessary as well as sufficient (see also our discussion following the figures).

In Figs. 1, 2 and 3 we consider the model problem (31)-DP1, with a splitting of the domain Ω into three subdomains. We present the contour plots of the experimentally determined number of iterations required to reduce the max norm of the difference of two successive iterants smaller than 10^{-5} as a function of the various relaxation parameters involved. The stars in these plots indicate the theoretically optimum relaxation parameters computed by using the formulas (13) and (26) (since there are only two interfaces) of the **ROB** and **AVE** methods, respectively. In all plots associated with the **AVE** method, we use $\gamma^2 = 2$. The Neumann relaxation parameters β_1 and β_2 are computed by formula (28) while we systematically vary the Dirichlet parameters α_1 and α_2 in $(0, 1)$. For the **ROB** method, we set $\gamma^2 = 2$ while the relaxation parameters vary in a larger interval since there are no bounds for them. For this method we see that there is a curve in the $\lambda_1\lambda_2$ plane with optimum values for the relaxation parameters.

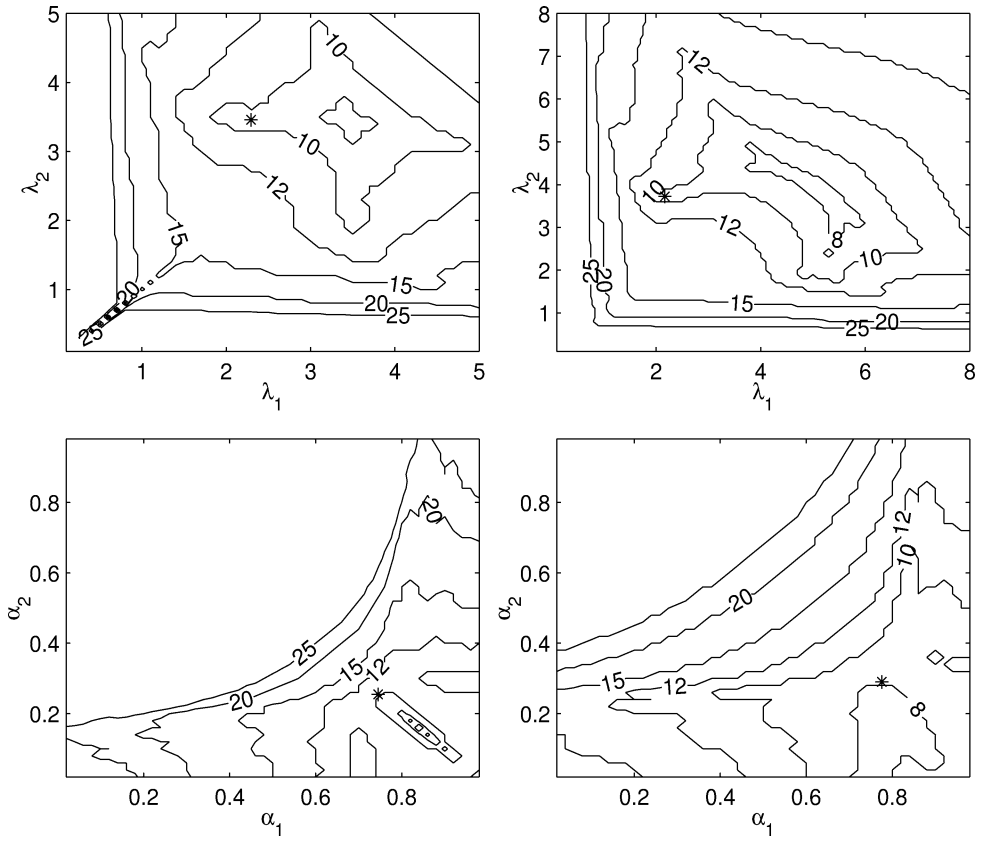

Fig. 1. Contour plots for case DP1 of the number of iterations required by the **ROB** (top two plots) and **AVE** (bottom two plots) methods to make the max norm of the difference of two successive iterants smaller than 10^{-5} as a function of associated relaxation parameters. We assume a uniform 3 subdomain partition in the graphs on the left and non-uniform partition with $x_1 = 0.2$ and $x_2 = 0.7$ on the right ($\gamma^2 = 2$). The star points are the theoretically determined optimum values of the parameters.

The stars in the **ROB** plots represent the optimum values computed using formula (13), which is located at the intersection of the above curve and the solution of Eq. (14) for $p = 3$, i.e.,

$$\lambda_1(\gamma_2 n_2 + \lambda_2 m_2) = \gamma_2(\gamma_2 m_2 + \lambda_2 n_2).$$

We note that, at the points indicated by stars in all the following graphs, the experimentally observed number of iterations are always in the range of 5 to 8. This confirms the theoretical optimality of the parameter values. It is also interesting to observe that this optimality seems to be independent of the uniformity of the decomposition and of the changes in the value of γ^2 in the subdomains.

In particular, in Fig. 2, we have the same non-uniform decomposition as in the right two plots in Fig. 1, but here the coefficient of u in the DE is discontinuous at the interface points. Specifically, in the first subdomain $\gamma^2 = 2$, in the second $\gamma^2 = 10$ and in the third $\gamma^2 = 4$. The right plot for **AVE**, is made using, as before, Neumann relaxation parameters (β_1, β_2) computed by formula (28) and letting α_1 and α_2 vary in $(0, 1)$.

In general, the **AVE** method seems to converge faster than **ROB** but Theorem 4 imposes a restriction on its convergence region. In Fig. 3 we experimentally verify the results of Theorem 4 and we clearly

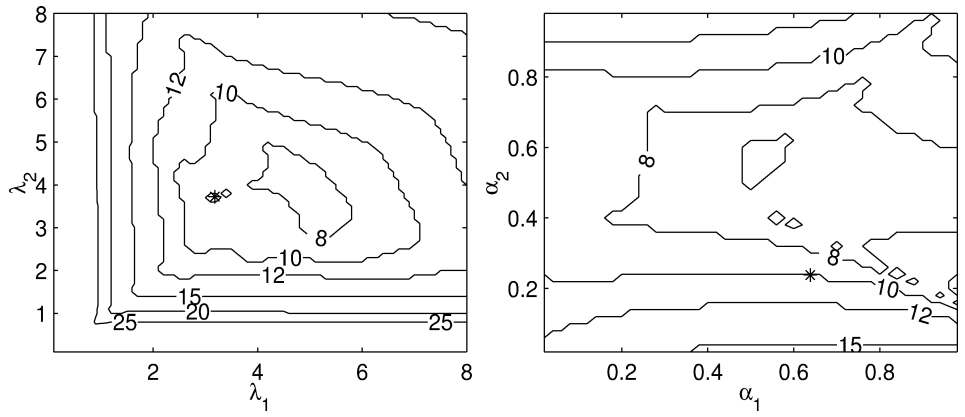

Fig. 2. Contour plots for case DP1 of the number of iterations required by the **ROB** (left) and the **AVE** (right) methods to make the max norm of the difference of two successive iterants smaller than 10^{-5} as a function of the associated relaxation parameters. We assume a non-uniform partition with $x_1 = 0.2$ and $x_2 = 0.7$, with a discontinuous coefficient of u. Particularly, $\gamma^2 = 2$ for the first subdomain, $\gamma^2 = 10$ for the second and $\gamma^2 = 4$ for the third subdomain. The stars represent the theoretical optimum values.

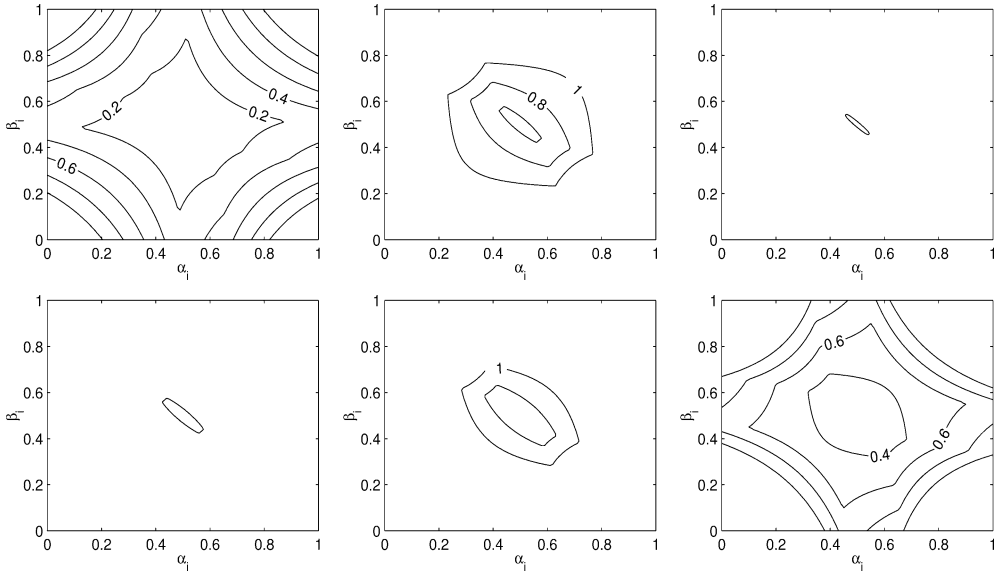

Fig. 3. Contour plots for case DP1 of the upper bounds of the spectral radius for the uniform case for the **AVE** method. In the top three plots $\gamma^2 = 20$ while the number of subdomains p is equal to 2 (left), 4 (middle) and 5 (right). In the bottom three figures we fix the number of subdomains at $p = 6$ and γ^2 is equal to 30 (left), 40 (middle) and 80 (right).

see that the restriction on the size of the subdomains imposed is not only sufficient but required, too. The restriction $\gamma \ell_i > \ln(1 + \sqrt{2})$ of Theorem 4 is, for the six cases in Fig. 3, for the top row ($\gamma/p = 2.24, 1.19, 0.89 > 0.881$) and bottom ($\gamma/p = 0.913, 1.05, 1.17 > 0.881$). The convergence region (the area where the spectral radius of the iteration matrix is less than 1) shrinks as one either increases the number of subdomains keeping γ^2 constant, or decreases γ^2 assuming a constant number

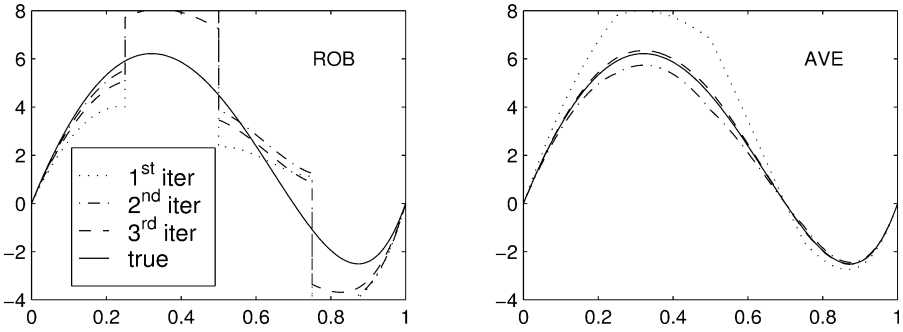

Fig. 4. Convergence history for case DP2 with $\gamma^2 = 20$ and a 4 subdomain uniform decomposition. The graph shows the true solution and the first three iterants for the **ROB** (on the left plot) and the **AVE** (on the right) methods.

of subdomains. The imposed bound on the size of subdomains seems to be a sharp one, since in all our experiments we observe divergence every time we make $\ell_i \gamma$ slightly less than $\ln(1+\sqrt{2})$ while we always observe convergence otherwise.

To obtain additional information on the convergence behavior of the two methods we now switch to the model problem (31)-DP2. The data for Figs. 4 and 5 have been extracted from [13] and are presented here for completeness. In Fig. 4 we set $\gamma^2 = 20$ and plot the true solution and the first three iterants. We observe that both methods converge in a non-monotone way, but **AVE** follows a much smoother path.

In Fig. 5, we consider the model problem (31)-DP2, with a two subdomain partition. We set all relaxation parameters equal to 0.5 and experimentally measure the effects that the size of γ^2 and the location of the interface point have on the convergence rates for the two methods. We plot the logarithm of the max norm of the error (on the y-axis) versus the number of iterations (on the x-axis). The interface point is fixed at 0.5 for the two plots on the left of the figure while $\gamma^2 = 20$ for the two on the right. We observe that the **AVE** method is significantly affected by both parameters while the **ROB** method converges in a smoother but slower way.

4.2. Two-dimensional case

We have implemented[3] the **AVE** and **ROB** methods for two-dimensional problems using ELLPACK [15] assuming "skyline" domains (a string of rectangles of different heights and widths). This leads to a one-dimensional decomposition of two-dimensional rectangles. The detailed presentation of this two-dimensional performance analysis is beyond the scope of this section but, we give an example in Fig. 6 of the convergence rate of the **AVE** and **ROB** methods. The Helmholtz differential equation is $-\Delta u + \gamma^2 u = f \in \Omega$ with Dirichlet boundary conditions where f is selected such that $u(x) = e^{y(x+4)}x(x-1)(x-0.7)y(y-0.5)$. The PDE domain and its one-dimensional partition into 3 subdomains is as follows:

$$\Omega_1 = (0, x_1) \times (0, 2), \qquad \Omega_2 = (x_1, x_2) \times (0, 0.5), \qquad \Omega_3 = (x_2, 1) \times (0, 1), \qquad \Omega \equiv \bigcap_{i=1}^{3} \Omega_i,$$

[3] See http://www.cs.purdue.edu/homes/giwta/dom-dec/2_dim/matlab/index.html.

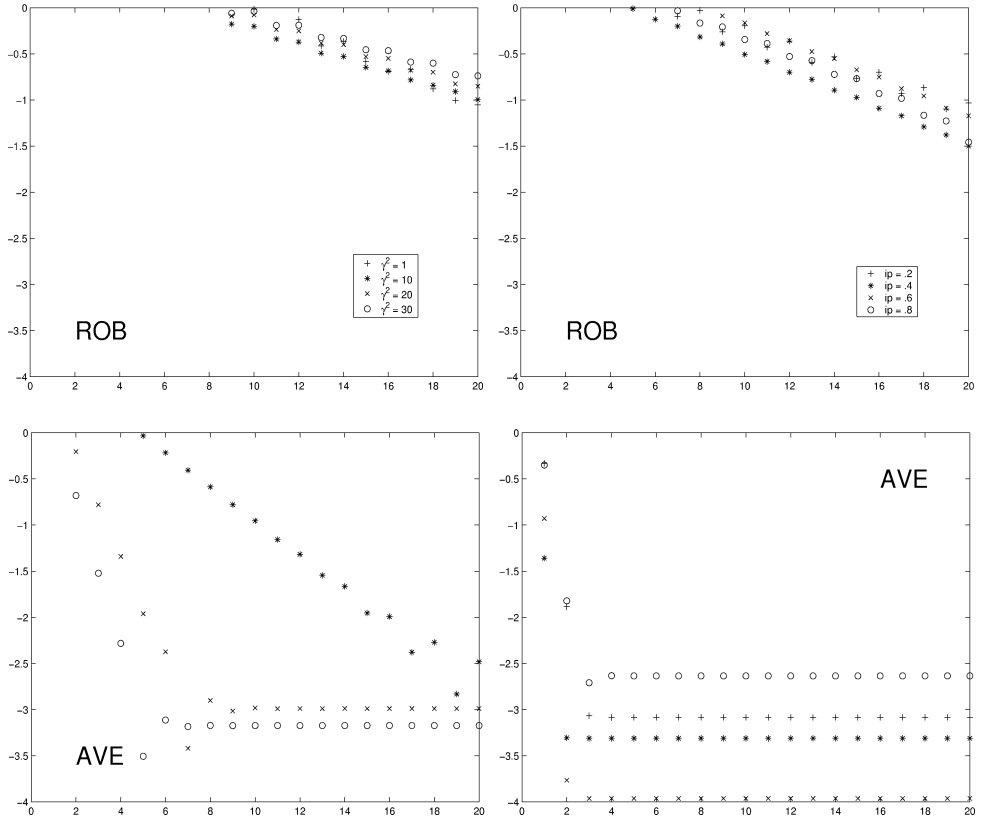

Fig. 5. The effect of the coefficient γ^2 (left graph, $\gamma^2 = 1, 10, 20, 30$) and of the location of the interface point (right, $x = 0.2, 0.4, 0.6, 0.8$) on the convergence rates for the **ROB** (top) and **AVE** (bottom) applied to case DP2. The y-axis is the max norm of the difference of successive solutions and the x-axis is the number of iterations.

where $0 < x_1 < x_2 < 1$. We have numerically verified that both the discretization scheme and the grid size have very little effect on the convergence rate of both the IR methods considered. In all the experiments associated with the present study the 5-point star ELLPACK discretization module was used and the domain is discretized with a uniform grid in both directions using $h = 0.01$.

The similarity of the convergence behavior between the one-dimensional and the two-dimensional problems is easily observed by comparing Figs. 1 and 6. We performed many other experiments (some of them are given in Chapter 6 in [20]), all of these were in reasonably good agreement with both the quantitative and qualitative conclusions we draw from the one-dimensional experiments presented above, provided that the subdomains are not very narrow in the y-direction. Specifically, it is apparent that the region of convergence shrinks down as the subdomains become large in the y-direction. This is consistent with the similar behavior observed or even proved in other conventional domain decomposition studies like [3].

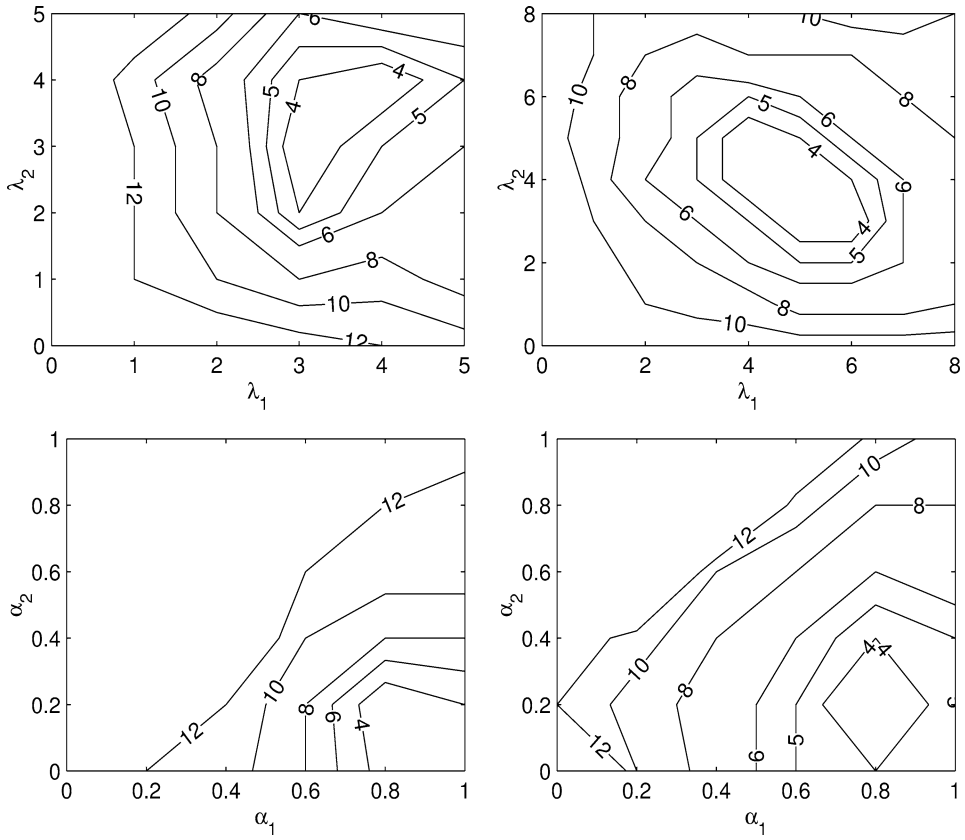

Fig. 6. Contour plots of number of iterations required for PDE problem defined in Section 4.2 by the **ROB** (top two plots) and **AVE** (bottom two plots) methods to make the max norm of the difference of two successive iterants smaller than 10^{-5} for the two-dimensional Dirichlet problem $-\Delta u + 2u = f$ as a function of associated relaxation parameters. We assume a uniform 3 subdomain partition in the graphs on the left and non-uniform partition with $x_1 = 0.2$ and $x_2 = 0.7$ on the right the PDE domain and its partition given on the left.

Acknowledgements

We are grateful to Prof. A. Hadjidimos for the constructive discussion which help us to derive the "optimum" values for the **ROB** method.

Appendix A. Analysis for the AVE method

A.1. Minimize the max-norm of M^D

The max-norm of M^D is given by

$$\left\| M^D \right\|_\infty = \max_{1 \leqslant i \leqslant p-1} f_i,$$

where

$$
\begin{aligned}
f_1(\alpha_1) &= \left|\frac{\alpha_1 m_1}{n_1\gamma_1} - \frac{(1-\alpha_1)n_2}{m_2\gamma_2}\right| + \frac{2(1-\alpha_1)}{m_2\gamma_2},\\
f_i(\alpha_i) &= \frac{2\alpha_i}{m_i\gamma_i} + \left|\frac{\alpha_i n_i}{m_i\gamma_i} - \frac{(1-\alpha_i)n_{i+1}}{m_{i+1}\gamma_{i+1}}\right| + \frac{2(1-\alpha_i)}{m_{i+1}\gamma_{i+1}}, \quad i = 2,\ldots,p-2,\\
f_{p-1}(\alpha_{p-1}) &= \frac{2\alpha_{p-1}}{m_{p-1}\gamma_{p-1}} + \left|\frac{\alpha_{p-1}n_{p-1}}{m_{p-1}\gamma_{p-1}} - \frac{(1-\alpha_{p-1})m_p}{n_p\gamma_p}\right|.
\end{aligned}
\tag{A.1}
$$

Considering the fact that $\gamma_i = \gamma,\ i = 1,\ldots,p$, as in Theorem 4, the formulas (A.1) can be simplified as

$$
\begin{aligned}
f_1(\alpha_1) &= \left|\frac{\alpha_1 m_1}{n_1\gamma} - \frac{(1-\alpha_1)n_2}{m_2\gamma}\right| + \frac{2(1-\alpha_1)}{m_2\gamma},\\
f_i(\alpha_i) &= \frac{2\alpha_i}{m_i\gamma} + \left|\frac{\alpha_i n_i}{m_i\gamma} - \frac{(1-\alpha_i)n_{i+1}}{m_{i+1}\gamma}\right| + \frac{2(1-\alpha_i)}{m_{i+1}\gamma}, \quad i = 2,\ldots,p-2,\\
f_{p-1}(\alpha_{p-1}) &= \frac{2\alpha_{p-1}}{m_{p-1}\gamma} + \left|\frac{\alpha_{p-1}n_{p-1}}{m_{p-1}\gamma} - \frac{(1-\alpha_{p-1})m_p}{n_p\gamma}\right|.
\end{aligned}
\tag{A.2}
$$

We present the analysis for the general case (i.e., for $f_i,\ i = 2,\ldots,p-2$). The minimum for f_1 and f_{p-1} is obtained in the same way.

The function f_i obtains its minimum value (see Fig. 7) at α_i^* or α_i^{**}, where α_i^* is the intersection point of the lines $\frac{2\alpha_i}{m_i\gamma}$ and $\frac{2(1-\alpha_i)}{m_{i+1}\gamma}$ and is equal to $\alpha_i^* = \frac{m_i}{m_i+m_{i+1}}$, while α_i^{**} is the root of the quantity in the absolute value, and is equal to $\alpha_i^{**} = \frac{m_i n_{i+1}}{m_{i+1}n_i + m_i n_{i+1}}$. Substituting α_i^* and α_i^{**} in f_i we get the following equalities

$$
f_i\left(\alpha_i^*\right) = \frac{4 + |n_i - n_{i+1}|}{\gamma(m_i + m_{i+1})},
\tag{A.3}
$$

and

$$
f_i\left(\alpha_i^{**}\right) = \frac{2(n_i + n_{i+1})}{\gamma(m_{i+1}n_i + m_i n_{i+1})}.
\tag{A.4}
$$

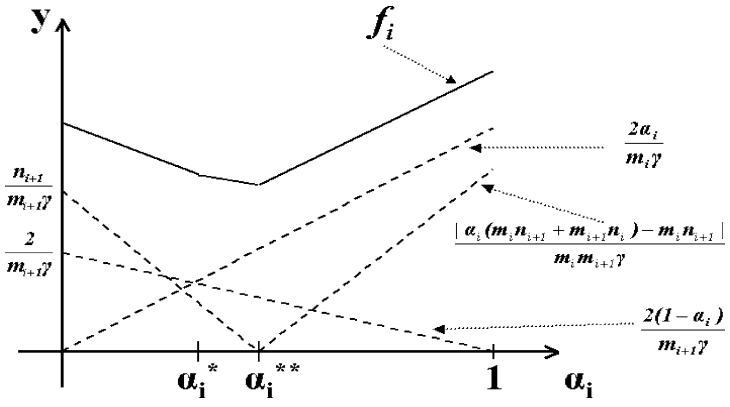

Fig. 7. The components of the sum of the absolute values of the elements of the ith row of matrix M^D.

Next, we compare the values in (A.3) and (A.4) and prove that $f_i(\alpha_i^{**})$ is the minimum. To do so, we show that the quantity $\gamma(f_i(\alpha_i^{**}) - f_i(\alpha_i^{*}))$ is negative under the assumption $n_i > 2,\ i = 1, \ldots, p-1$. It is easy to see that

$$f_i^* \equiv \gamma\big(f_i\big(\alpha_i^{**}\big) - f_i\big(\alpha_i^{*}\big)\big) = \frac{2(m_{i+1} - m_i)(n_{i+1} - n_i) - |n_{i+1} - n_i|(m_{i+1}n_i + m_i n_{i+1})}{(m_i + m_{i+1})(m_{i+1}n_i + m_i n_{i+1})}.$$

We derive two cases with respect to the difference in the absolute value and we have that

$$f_i^* = \begin{cases} (n_{i+1} - n_i)\big(m_{i+1}(n_i + 2) + m_i(n_{i+1} - 2)\big), & n_i > n_{i+1}, \\ -(n_{i+1} - n_i)\big(m_{i+1}(n_i - 2) + m_i(n_{i+1} + 2)\big), & n_i \leqslant n_{i+1}. \end{cases}$$

In the first branch, where $n_i > n_{i+1}$, the quantity in the second parenthesis is positive under the assumption that $n_i > 2$ and therefore f_i^* is negative, while in the second branch the first parenthesis is positive and the second one is negative assuming that $n_{i+1} > 2$.

Hence, under the constraint $n_i > 2,\ i = 1, \ldots, p-1$ (which is equivalent to the only constraint of Theorem 4), we have proved that $f_i(\alpha_i^{**}) < f_i(\alpha_i^{*})$, which makes α_i^{**} the minimum of the function f_i.

A.2. Minimize the max-norm of M^N

The max-norm of M^N is given by

$$\big\|M^N\big\|_\infty = \max_{1 \leqslant i \leqslant p-1} g_i,$$

where

$$\begin{aligned} g_1(\beta_1) &= \left|\frac{\beta_1 n_1 \gamma_1}{m_1} - \frac{(1-\beta_1)n_2\gamma_2}{m_2}\right| + \frac{2(1-\beta_1)\gamma_2}{m_2}, \\ g_i(\beta_i) &= \frac{2\beta_i\gamma_i}{m_i} + \left|\frac{\beta_i n_i \gamma_i}{m_i} - \frac{(1-\beta_i)n_{i+1}\gamma_{i+1}}{m_{i+1}}\right| + \frac{2(1-\beta_i)\gamma_{i+1}}{m_{i+1}}, \quad i = 2, \ldots, p-2, \\ g_{p-1}(\beta_{p-1}) &= \frac{2\beta_{p-1}\gamma_{p-1}}{m_{p-1}} + \left|\frac{\beta_{p-1}n_{p-1}\gamma_{p-1}}{m_{p-1}} - \frac{(1-\beta_{p-1})n_p\gamma_p}{m_p}\right|. \end{aligned} \tag{A.5}$$

Working in the same way as in the previous section, we prove that the $\beta_i,\ i = 1, \ldots, p-1$, as defined in (28) and (29) are the optimum values, in the sense that they minimize the max-norm of matrix M^N.

References

[1] P.E. Bjørstad, O.B. Widlund, Iterative methods for the solution of elliptic problems on regions partitioned into substructures, SIAM J. Numer. Anal. 23 (6) (1986) 1093–1120.
[2] J.H. Bramble, J.E. Pasciak, A.H. Schatz, An iterative method for elliptic problems on regions partitioned into substructures, Math. Comp. 46 (173) (1986) 361–369.
[3] T. Chan, T. Hou, P.L. Lions, Geometry related convergence results for domain decomposition algorithms, SIAM J. Numer. Anal. 28 (1991) 378–391.
[4] Q. Deng, An analysis for a nonoverlapping domain decomposition iterative procedure, SIAM J. Sci. Comput. 18 (1997) 1517–1525.
[5] B. Despres, Méthodes de décomposition de domaines pour les problèmes de propagation d'ondes en régime harmonique, Ph.D. Thesis, Université Paris IX Dauphine, UER Mathématiques de la Decision, Paris, 1991.

[6] A. Hadjidimos, D. Noutsos, M. Tzoumas, Nonoverlapping domain decomposition: A linear algebra viewpoint, Math. Comput. Simulation 51 (1999) 597–625.
[7] J. Douglas Jr., C.-S. Huang, An accelerated domain decomposition procedure based on Robin transmission conditions, Technical report, Purdue University, Department of Mathematics, 1996.
[8] J. Douglas Jr., P.J. Paes Leme, J.E. Roberts, J. Wang, A parallel iterative procedure applicable to the approximate solution of the second order partial differential equations by mixed finite element methods, Numer. Math. 65 (1993) 95–108.
[9] S.-B. Kim, A. Hadjidimos, E.N. Houstis, J.R. Rice, Multi-parameterized Schwarz splittings, Math. Comput. Simulation 42 (1996) 47–76.
[10] P.L. Lions, On the Schwarz alternating method III: A variant for nonoverlapping subdomains, in: R. Glowinski, G.H. Golub, G.A. Meurant, J. Periaux (Eds.), Domain Decomposition Methods for Partial Differential Equations, SIAM, Philadelphia, PA, 1990, pp. 202–223.
[11] M. Mu, Solving composite problems with interface relaxation, SIAM J. Sci. Comput. 20 (1999) 1394–1416.
[12] M. Mu, J.R. Rice, Modeling with collaborating PDE solvers—Theory and practice, Comput. Systems in Engrg. 6 (1995) 87–95.
[13] J.R. Rice, P. Tsompanopoulou, E.A. Vavalis, Interface relaxation methods for elliptic differential equations, Appl. Numer. Math. 32 (2000) 219–245.
[14] J.R. Rice, An agent–based architecture for solving partial differential equations, SIAM News 31 (1998).
[15] J.R. Rice, R.F. Boisvert, Solving Elliptic Problems Using ELLPACK, Springer, New York, 1985.
[16] J.R. Rice, P. Tsompanopoulou, E. Vavalis, Automated estimation of relaxation parameters for interface relaxation, Technical Report CSD-TR-98-018, Purdue University, Computer Science Department, 1998.
[17] J.R. Rice, E. Vavalis, D. Yang, Analysis of a non-overlapping domain decomposition method for elliptic PDEs, J. Comput. Appl. Math. 87 (1997) 11–19.
[18] Y.-H. De Roeck, P. Le Tallec, Analysis and test of a local domain decomposition preconditioner, in: R. Glowinski, Y. Kuznetsov, G. Meurant, J. Périaux, O. Widlund (Eds.), Fourth International Symposium on Domain Decomposition Methods for Partial Differential Equations, SIAM, Philadelphia, PA, 1991.
[19] P. Le Tallec, Y.-H. De Roeck, M. Vidrascu, Domain-decomposition methods for large linearly elliptic three dimensional problems, J. Comput. Appl. Math. 34 (1991).
[20] P. Tsompanopoulou, Collaborative PDEs solvers: Theory and practice, Ph.D. Thesis, Mathematics Department, University of Crete, Greece, 2000.
[21] H.T.M. van der Maarel, A. Platschorre, Optimization of flexible computing in domain decomposition for a system of PDEs, in: P. Biørstad, M. Espedal, D. Keyes (Eds.), Proc. of the Ninth International Conference on Domain Decomposition Methods, Wiley, New York, 1998.
[22] R.S. Varga, Matrix Iterative Analysis, Prentice-Hall, Englewood Cliffs, NJ, 1962 (2nd Edition revised and expanded, Springer, Berlin, 2000).
[23] O.B. Widlund, Some Schwarz methods for symmetric and nonsymmetric elliptic problems, in: T.F. Chan, D.E. Keyes, G.A. Meurant, J.S. Scroggs, R.G. Voigt (Eds.), Fifth International Symposium on Domain Decomposition Methods for Partial Differential Equations, SIAM, Philadelphia, PA, 1992.
[24] D. Yang, A parallel iterative nonoverlapping domain decomposition procedure for elliptic problems, IMA J. Numer. Anal. 16 (1996) 75–91.
[25] D. Yang, A parallel domain decomposition algorithm for elliptic problems, J. Comput. Math. 16 (1998) 141–151.
[26] D. Yang, A parallel grid modification and domain decomposition algorithm for local phenomena capturing and load balancing, J. Sci. Comput. 12 (1998) 99–117.